Comparative first- and second-law parametric study of transient diesel engine operation

C.D. Rakopoulos*, E.G. Giakoumis

Internal Combustion Engines Laboratory, Department of Thermal Engineering, School of Mechanical Engineering, National Technical University of Athens, Zografou Campus, 9 Heroon Polytechniou Str., 15780 Athens, Greece

Abstract

A computer model is developed for studying the first- and second-law (availability) balances of a turbocharged diesel engine, operating under transient load conditions. Special attention is paid to the direct comparison between the results from the two laws, for various operating parameters of the engine. The model simulates the transient operation on a degree crank angle basis, using a detailed analysis of mechanical friction, a separate consideration for the processes of each cylinder during a cycle (''multi-cylinder'' model) and a mathematical model of the fuel pump. Experimental data taken from a marine duty, turbocharged diesel engine, located at the authors' laboratory, are used for the evaluation of the model's predictive capabilities. The first-law (e.g., engine speed, fuel pump rack position, engine load, etc.) and second-law (e.g., irreversibilities, heat loss and exhaust gases) terms for the diesel engine cylinder are both computed and depicted in comparison, using detailed diagrams, for various engine operating parameters. It is revealed that, at least for the specific engine type and operation, a thermodynamic, dynamic or design parameter can have a conflicting impact on the engine transient response as regards energy and availability properties, implying that both a first- and second-law optimization is needed for best performance evaluation.
© 2005 Elsevier Ltd. All rights reserved.

Keywords: Transient analysis; First law; Second law; Parametric study

1. Introduction

The transient response of turbocharged diesel engines forms a significant part of their operation and is often characterized by short but serious off-design functions, requiring careful and proper modeling for successful study of the speed response. Transient diesel engine modeling extends from quasi-linear codes [1] using experimental data at steady-state conditions together with dynamic equations for the engine, turbocharger and governor, to a more advanced work where the simulation is based on a detailed thermodynamic (per degree crank angle (CA)) analysis [2–10].

On the other hand, during the last two decades, it has become clear that second-law (availability) analysis, with detailed study of what is happening during a process, has contributed a new way of thinking about and

*Corresponding author. Fax: +30 210 7723531.

E-mail address: cdrakops@central.ntua.gr (C.D. Rakopoulos).

Nomenclature

A	availability (J)
b	flow availability (J/kg)
G	mass moment of inertia (kg m^2), or Gibbs free enthalpy (J)
h	specific enthalpy (J/kg)
I	irreversibility (J)
m	mass (kg)
$\dot{m}$	mass flow rate (kg/s)
N	engine speed (rpm)
p	pressure (Pa)
Q	heat (J)
S	entropy (J/K)
T	absolute temperature (K), or torque (N m)
t	time (s)
U	internal energy (J)
V	volume (m^3)
z	fuel pump rack position (m)

Greek symbols

φ	crank angle (deg or rad)
ω	angular velocity (s^{-1})

Subscripts

0	reference conditions
1	cylinder inlet (inlet manifold conditions)
2	cylinder outlet (in-cylinder conditions)
ch	chemical
e	engine
f	fuel
fb	fuel burning
fr	friction
g	gas
j	any cylinder
L	load or loss
tot	total
w	wall or work

Abbreviations

°CA	degrees of crank angle
rpm	revolutions per minute
T/C	turbocharger

studying various thermodynamic engine processes [11–24]. In particular, second law introduces the term of irreversibilities, the reduction of which can lead to better engine performance through the possible recovery of the work potential in the exhaust gases or heat losses. The increasing oil prices during the very last years have

yet again raised the demand for reduced fuel consumption and it is believed that in order to achieve this goal, apart from the traditional first-law analysis, the second-law analysis can contribute a lot.

Various second-law analyses have been reported in the past concerning internal combustion engines [12,14,17–22]. For example, Van Gerpen and Shapiro [18] applied a detailed second-law balance investigating also the effect of combustion timing, shape of heat release curve and heat correlation parameters. The irreversibilities production mechanism has been studied in [12,15,19,23], the entropy generation in [25] and various parametric studies have also been reported [18,24]. However, the second-law transient operation has been dealt with only by the present research group in Ref. [26] as regards naturally aspirated and in Refs. [27,28] as regards turbocharged diesel engines.

Many studies in the past have focused on the direct comparison between first- and second-law properties of the (turbocharged) diesel engine operating at steady-state conditions [12,14,17,19]. Alkidas [12,22] conducted a comparative first- and second-law analysis, on an overall basis, for a single cylinder, open chamber diesel engine at two different engine speeds. Flynn et al. [17] focused on the turbocharged diesel engine operation, on a degree CA basis, with special reference to the combustion process and the insulation of the cylinder walls. Bozza et al. [14] carried out a comparative first- and second-law study too, which also included various efficiencies evaluation, again on a degree CA basis. However, all of the above models were applied to the steady-state operation of the internal combustion engine.

In this paper, we extend the comparative first- and second-law analysis of the previous researchers to the transient operation of the turbocharged diesel engine, including various engine operating parameters effects. By so doing, we are able to establish possible differentiations in the results given by the two thermodynamic laws, during transient response after a ramp increase in load. This can serve as a significant guide towards a better understanding of the engine processes.

A transient diesel engine simulation code, based on the filling and emptying modeling technique, has been developed, which incorporates some important features to account for the peculiarities of the transient operations. Relations concerning (indirect) fuel injection, combustion, dynamic analysis, heat transfer to the cylinder walls, friction modeling and fuel pump operation during the transient response have been developed [6,7,9]. Moreover, a "multi-cylinder" engine model is incorporated, i.e., one which solves the corresponding differential equations individually for each cylinder, providing a more detailed simulation of the transient processes. The latter issue is important since, during a transient event, considerable differentiations in fueling from cylinder to cylinder inside the same cycle are observed, mainly during the first cycles.

The experimental investigation was carried out on a six-cylinder, IDI (indirect injection), turbocharged and aftercooled, medium–high speed diesel engine of marine duty, coupled to a hydraulic brake, located at the authors' laboratory. A high-speed data acquisition system was set up for measuring engine and turbocharger variables performance, under both steady-state and transient operation. The transient behavior of the engine is predicted adequately by the developed code, despite the long non-linear brake loading times and the indirect fuel injection nature of the engine in hand.

The availability balance equation is applied to the present diesel engine cylinder. Various availability properties developed during a transient event such as work, heat transfer, exhaust gas (from cylinder or to ambient) and in-cylinder irreversibilities are depicted in detailed multiple diagrams in comparison to their important first-law counterparts, i.e., engine speed, fuel pump rack position, turbocharger speed, engine load and manifolds' pressures and temperatures. The analysis covers a wide range of engine thermodynamic, dynamic and design parameters, such as type of load (resistance) connected to the engine, turbocharger mass moment of inertia, cylinder wall insulation, aftercooler effectiveness and exhaust manifold volume.

2. First-law analysis

2.1. General process description

Since the present analysis does not include prediction of exhaust gases emissions and on the other hand it deals with transient operation calculations on a degree CA basis, a single-zone model is used as the basis for the thermodynamic processes evaluation. This approach combines satisfactory accuracy with limited computer program execution time. The (domestic) diesel fuel used is considered to have the properties of

dodecane ($C_{12}H_{26}$) with a lower heating value of 42.5 MJ/kg. Perfect gas behavior is assumed. Polynomial expressions from Ref. [29] with 0 K reference datum are used for each of the four species (O_2, N_2, CO_2, and H_2O) considered. They concern the evaluation of internal energy and specific heat capacities for first-law application to the cylinder contents, using the filling and emptying modeling technique on a degree CA basis [1,19,29–32].

2.2. Combustion model

For studying the combustion process, the model proposed by Whitehouse and Way [30] is used for both the main chamber and the prechamber of the IDI engine in hand. In this model the combustion process consists of two parts, i.e., a preparation-limited and a reaction-limited combustion rate. Details about the governing equations can be found in Refs. [1,6,19,27,30].

For a proper simulation of transient response, it is vital that the combustion modeling takes into consideration the continuously changing nature of operating conditions. Thus, the constant K_1, in the (dominant) preparation rate equation of the Whitehouse–Way model, is correlated with the Sauter mean diameter (SMD) of the fuel droplets through a formula of the type $K_1 \propto (1/\text{SMD})^2$ [30] for both chambers of the engine. For the evaluation of SMD (in μm), the empirical expression proposed by Hiroyasu et al. [33] is used:

$$\text{SMD} = 25.1(\Delta p)^{-0.135} \rho_g^{0.12} V_{\text{tot}}^{0.131}, \tag{1}$$

where Δp is the mean pressure drop across the injection nozzle in MPa (derived from the fuel pump sub-model described later), ρ_g is the density of air in kg/m^3 at the time the injection starts, and V_{tot} is the amount of fuel delivered per cylinder and per cycle in mm^3.

2.3. Heat transfer model

The model of Annand [34] is used to simulate the heat loss Q_L to the cylinder walls,

$$\mathrm{d}Q_L/\mathrm{d}t = F[a\lambda \, \text{Re}^b (T_w - T_g)/D + c(T_w^4 - T_g^4)], \tag{2}$$

where $F = \pi D^2/2 + \pi D x$, is the surface of the main chamber with x the instantaneous cylinder height [29] in contact with the gas.

The temperature T_w used above corresponds to the cylinder liner, with $\pi D x$ being the surface needed in Eq. (2). For the piston crown, the temperature is always assumed to be 50 K higher (corresponding surface $\pi D^2/4$) and for the cylinder head (corresponding surface $\pi D^2/4$) the temperature is assumed to be 100 K higher than the current one of the liner, at each degree CA. Prechamber wall temperature is also assumed to be 100 K higher than the corresponding liner one.

For transient operation, a hysterysis (time lag due to inertia) expression is developed to update the wall temperature T_w at each consecutive cycle, which changes (at a very slow rate) as a result of the increase in speed and/or fueling, i.e.,

$$T_w = T_{wo} + \Delta T_w (1 - e^{-d_t t}). \tag{3}$$

In Eq. (3), d_t is a coefficient determining how "fast" or how "slow" the wall temperature responds to the changes in fueling, a fact depending on the wall insulation used. T_{wo} is the initial wall temperature and $\Delta T_w = (T_{wst} - T_{wo})$, with T_{wst} the instantaneous steady-state wall temperature according to the current engine fueling. The analysis assumes that throughout each cycle the wall temperature has a constant value, differentiating from cycle to cycle according to Eq. (3).

2.4. Friction model

Transient simulation codes have always in the past used "mean fmep" (friction mean effective pressure) relations to model the friction torque inside the cylinder. These have the obvious drawback of considering that friction torque remains steady throughout each cycle. In the present analysis, we adapt the method proposed

by Rezeka and Henein [35], which describes the non-steady profile of friction torque during a cycle. In this method the total amount of friction is divided into six parts, i.e., ring viscous lubrication, ring mixed lubrication, piston skirt, valve train, auxiliaries and journal bearings. The important aspect about this method is that friction torque varies during each degree CA in the engine simulation. Moreover, using the "multi-cylinder" model described in the next subsection, we are able to calculate the friction torque terms separately for each cylinder at each computational step.

2.5. Multi-cylinder model

At steady-state operation, the performance of each cylinder is essentially the same, due to the steady-state functioning of the governor clutch resulting in the same amount of fuel injected per cycle. At transient operation, on the contrary, each cylinder experiences different fueling and air mass flow rate during the same engine cycle, because of the continuous movement of the fuel pump rack initiated by the load or speed change. These differentiations in fueling and air mass flow rate may result in significant differentiations in torque response and finally speed, primarily during the early cycles, thus affecting significantly the whole engine operation.

Therefore, for the proper simulation of transient engine performance, a "multi-cylinder" engine model is developed, i.e., one in which all the governing differential and algebraic equations are solved individually and sequentially for every one cylinder of the six-cylinder engine concerned. Furthermore, with this model, a more accurate simulation of the manifolds' processes is achieved even at steady-state operation.

2.6. Fuel pump model

The amount of fuel injected per cycle and cylinder is found according to the instantaneous values of engine speed and fuel pump rack position, existing at the point of static injection timing of the particular cylinder. To this aim, a mathematical fuel injection model is used to simulate the fuel pump [36] taking into account the delivery valve and injector needle motion. The unsteady gas flow equations are solved using the method of characteristics, which provides the dynamic injection timing as well as the duration and the rate of injection for each cylinder at each transient cycle. This constitutes a vital improvement in transient modeling, since the fueling characteristics during a transient event differ broadly from the steady-state curves.

3. Second-law analysis

The availability of a system in a given state is defined as the maximum reversible work that can be produced through interaction of the system with its surroundings as it reaches thermal, mechanical and chemical equilibrium [11].

The present thermodynamic analysis, as based on a single zone approach, deals only with the four basic gas constituents (no dissociation is taken into account), which are also present in the environment, so there are no partial products in the exhaust that could be either oxidized or reduced. Moreover, the work that could be obtained (with the use of semi-permeable membranes or other special devices such as the Van't Hoff cells) due to the difference in the partial pressures between the system constituents at the dead state and their surrounding counterparts is practically not applicable [14,17]. Thus, for the present study, only thermal and mechanical availability terms are taken into account, while chemical availability is involved only as far as the reaction of fuel to form products is concerned. Further, since this study concerns a diesel engine (overall lean conditions), in the real case there are practically no partial products in the exhaust gases that could contain substantial chemical availability. The environmental (i.e., dead state) pressure and temperature conditions are $p_0 = 1$ bar and $T_0 = 298.15$ K, while the dead state molar composition is 20.35% O_2, 76.59% N_2, 0.03% CO_2 and 3.03% H_2O.

In the following subsections, the availability balance equation will be applied to the cylinder of the diesel engine, on a degree CA basis [19].

The cylinder availability balance reads:

$$\frac{\mathrm{d}A_j}{\mathrm{d}\varphi} = \frac{\dot{m}_{1j}b_{1j} - \dot{m}_{2j}b_{2j}}{6N} - \frac{\mathrm{d}A_\mathrm{w}}{\mathrm{d}\varphi} - \frac{dA_\mathrm{L}}{d\varphi} + \frac{\mathrm{d}A_f}{\mathrm{d}\varphi} - \frac{\mathrm{d}I}{\mathrm{d}\varphi} \tag{4}$$

with $\dot{m}_{1j}$ the incoming flow rate from the inlet manifold and $\dot{m}_{2j}$ the outgoing one to the exhaust manifold for cylinder "j" according to the first-law analysis, while it holds $\mathrm{d}\varphi = 6N\mathrm{d}t$ with N the engine speed in rpm and $\mathrm{d}\varphi$ in degrees CA;

$$\frac{\mathrm{d}A_\mathrm{w}}{\mathrm{d}\varphi} = (p_{2j} - p_0)\frac{\mathrm{d}V}{\mathrm{d}\varphi} \tag{5}$$

is the work transfer, where $\mathrm{d}V/\mathrm{d}\varphi$ is the rate of change of cylinder volume with CA [19,29] and p_{2j} the instantaneous cylinder pressure;

$$\frac{\mathrm{d}A_\mathrm{L}}{\mathrm{d}\varphi} = \frac{\mathrm{d}Q_\mathrm{L}}{\mathrm{d}\varphi}\left(1 - \frac{T_0}{T_{2j}}\right) \tag{6}$$

is the heat transfer to the cylinder walls with $\mathrm{d}Q_\mathrm{L}/\mathrm{d}\varphi$ (considered here as external to the cylinder control volume unlike, e.g., Alkidas [12,22] who treated the heat losses as a source of irreversibility) given by the Annand correlation, and T_{2j} the instantaneous gas temperature of cylinder j;

$$\frac{\mathrm{d}A_f}{\mathrm{d}\varphi} = \frac{\mathrm{d}m_{fb}}{\mathrm{d}\varphi}a_\mathrm{fch} \tag{7}$$

is the burned fuel m_{fb} availability, with a_fch the (chemical) availability associated with burning liquid hydrocarbon fuels of the type C_mH_n, given by Moran [11]:

$$a_\mathrm{fch} = \mathrm{LHV}[1.04224 + 0.011925(n/m) - 0.042/m]. \tag{8}$$

For the present analysis, $m = 12$, $n = 26$, so $a_\mathrm{fch} = 1.064\,\mathrm{LHV}$. The fuel burning rate $\mathrm{d}m_{fb}/\mathrm{d}\varphi$, for each chamber and for each computational step, is calculated using the model of Whitehouse–Way. The term on the LHS of Eq. (4) is expressed explicitly as

$$\frac{\mathrm{d}A_j}{\mathrm{d}\varphi} = \frac{\mathrm{d}U_j}{\mathrm{d}\varphi} + p_0\frac{\mathrm{d}V_j}{\mathrm{d}\varphi} - T_0\frac{\mathrm{d}S_j}{\mathrm{d}\varphi} - \frac{\mathrm{d}G_{0j}}{\mathrm{d}\varphi}, \tag{9}$$

representing the change in the availability of the contents of cylinder j under consideration. Details about the derivation of terms U, S, and G can be found in Ref. [27], with a 0 K temperature reference datum being used.

The terms b_{1j} and b_{2j} in Eq. (4) refer to the flow availability of the incoming and the outgoing cylinder mass flow rate, respectively, defined as (only thermomechanical availability considered) [11]

$$b = h - h_0 - T_0(s - s_0). \tag{10}$$

The term $\mathrm{d}I/\mathrm{d}\varphi$ in Eq. (4) is the rate of irreversibility production within the cylinder consisting mainly of the combustion term, while inlet-valve throttling and mixing of the incoming air with the cylinder residuals contribute not more than 5% of the total [27].

4. Dynamic analysis

If G_tot represents the total system moment of inertia (engine, flywheel and load), then the conservation of energy principle applied to the total system (engine plus load) yields [1,2,9]:

$$T_\mathrm{e}(\varphi, \omega) - T_\mathrm{L}(\omega) - T_\mathrm{fr}(\varphi, \omega) = G_\mathrm{tot}(\mathrm{d}\omega/\mathrm{d}t), \tag{11}$$

where $T_\mathrm{e}(\varphi, \omega)$ stands for the instantaneous value of the engine torque consisting of the gas and the inertia forces torque. Also, $T_\mathrm{L}(\omega)$ is the load torque,

$$T_\mathrm{L}(\omega) \propto \omega^s. \tag{12}$$

For the hydraulic brake coupled to the engine examined, $s = 2$. Lastly, $T_\mathrm{fr}(\varphi, \omega)$ stands for the friction torque, which varies during each cycle and for every cylinder according to the explicit friction analysis based

on the Rezeka–Henein [35] method (see Section 2.4 above). Both engine and friction torque terms in Eq. (11) are computed, at each calculation step, summing up each one cylinder's contribution.

5. Solution of equations

All the energy equations are solved for every $1/4°$CA for the closed part of each cycle, or every $1/2$ °CA for the open part, and for each engine cylinder. The dynamic and the availability equations are solved once every degree CA. These computational steps were found to be adequate for the particular engine–turbocharger–brake configuration, which is characterized by a high-mass moment of inertia.

6. Experimental procedure

The objective of the experimental test bed developed was to validate the transient performance of the engine simulation by setting up a comprehensive instrumentation. The experimental investigation was conducted on an MWM TbRHS 518S, six-cylinder, turbocharged and aftercooled, IDI, medium-high speed diesel engine of marine duty. The engine is fitted with a "KKK" turbocharger, a water aftercooler after the turbocharger compressor and is permanently coupled to a "Schenck" hydraulic dynamometer. Details about the experimental setup can be found in Ref. [7]. The basic data for the engine, turbocharger, brake and data processing system are given in Table 1.

The first requirement from the engine test bed instrumentation was to investigate the steady-state performance of the engine in question. For this purpose, an extended series of steady-state trials was conducted, in order on the one hand to examine the model's predictive capabilities and on the other to calibrate successfully the individual sub-models. By so doing, the constants for the combustion, heat transfer, friction and fuel pump simulation was made possible to be determined.

The investigation of transient operation was the next task. Since the particular engine is one with a relatively small speed range, mainly load changes (increases) with constant governor setting were examined. For the transient tests conducted, the initial speed was 1180 or 1380 rpm and the initial load 10% of the engine full load. The final conditions for the transient events varied from 47% to 95% of the engine full load, as analyzed in detail in Ref. [7].

A typical example of a conducted transient experiment is given in Fig. 1, showing the response of some important first-law properties. Here, the initial load was 10% of the full engine load at 1180 rpm. The final load applied was almost 75% of the full engine load (650% load change). The application of the final load was effected by the movement of the brake control lever (this task lasted 0.2 s), which in turn increased the amount of water inside the brake by appropriately increasing the active surface of the inlet tube. However, this hydraulic brake is characterized by a high-mass moment of inertia, in the order of 5.375 kg m^2, resulting in long and non-linear actual load-change times. This phenomenon was accounted for in the simulation model by arbitrarily increasing the load application time. The overall matching between experimental and predicted

Table 1
Basic data for engine, turbocharger, dynamometer and data logging system

|	
Engine model and type	MWM TbRHS 518S In-line, 6-cyl., 4-stroke, compression ignition, IDI, turbocharged, aftercooled, marine duty
Speed range	1000–1500 rpm
Bore/stroke	140 mm/180 mm
Compression ratio	17.7
Maximum power	320 HP (236 kW) @ 1500 rpm
Maximum torque	1520 N m @ 1250 rpm
Total moment of inertia (engine, flywheel and brake)	15.60 kg m^2
Turbocharger moment of inertia	7.5×10^{-4} kg m^2
Data logging system	Two 12-bit, 8-channel ADCs, 100 kHz max. sampling rate, installed on IBM compatible PCs
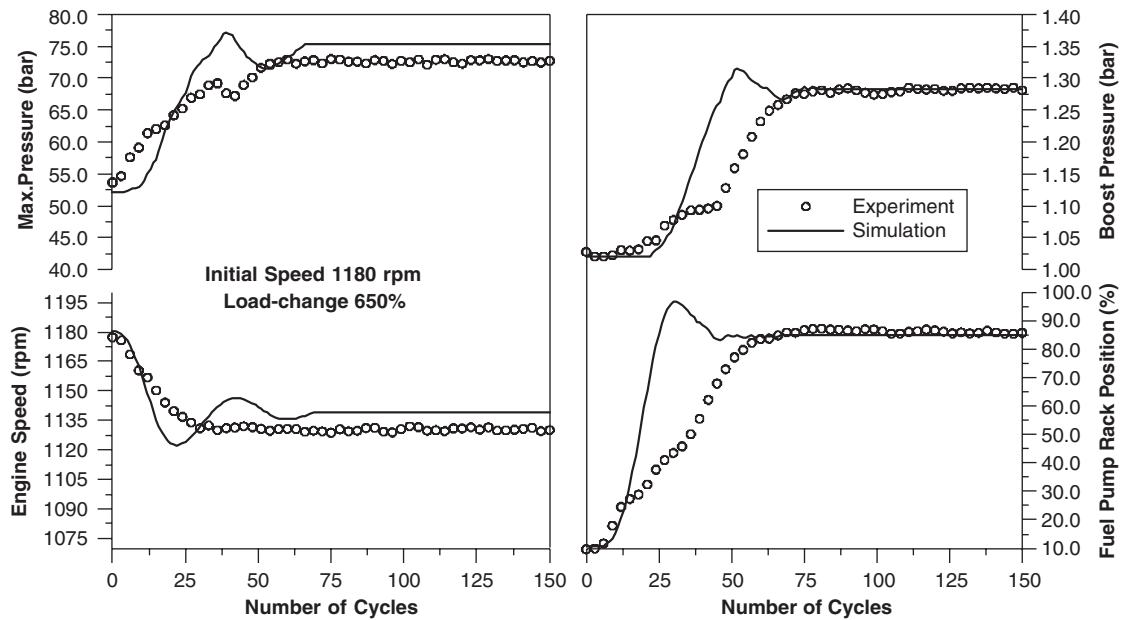
Fig. 1. Predicted and experimental engine energy response to an increase in load.

transient responses seems to be satisfactory for both engine and turbocharger variables (engine speed, maximum pressure for main chamber, fuel pump rack position and boost pressure) as regards final operating conditions of the transient test. The fuel pump rack position is notably delayed compared to the speed profile, due to the hysterysis effect induced by the governor. Boost pressure and, mainly, main chamber maximum pressure are closely correlated to the fuel pump rack position response.

7. Comparison between first- and second-law results of transient operation

Fig. 2 shows the response of the in-cylinder availability terms, viz., work, heat loss to the walls, exhaust gas and irreversibilities as a function of the engine cycles. All of these terms are cumulative values (in Joules) over each cycle (for all six cylinders of the engine). The availability term for work and heat loss to the walls increase with fueling as a function of the engine cycles, because of increases in the charge temperature resulting from increases of the injected fuel quantity and accompanying fuel–air equivalence ratios. Similar results hold for the exhaust gas from the cylinder term and for the irreversibilities term. Cylinder irreversibilities consist of combustion ones (almost 95% of the total), inlet and exhaust ones. The engine speed response is also depicted for comparative purposes. All availability terms are characterized by a time delay compared to the engine speed (cf. Fig. 1), while the in-cylinder irreversibilities follow closely the profile of the injected fuel (availability) highlighting their main contributor. Due to the moment of inertia of the engine-load setup being 2–3 times higher than the usual configurations, no significant differentiations were observed from cycle to cycle between the individual cylinders during a transient test. Therefore, the general profile of the contribution of all cylinders' availability terms, presented in Fig. 2, is very close to the profile obtained if only the results from one cylinder were taken into account.

In Fig. 2, a comparison is also included between transient and some intermediate "steady-state" irreversibilities terms (i.e., steady-state irreversibilities at the engine speed and fueling of the corresponding transient cycles). A difference up to 11% at the 20th cycle is observed highlighting the different evolution profile of transient combustion irreversibilities compared to steady-state operation.

Fig. 3 examines the same in-cylinder properties, but now their values are reduced to the cylinder's fuel availability over each cycle. Here, we can see that the reduced availability term for heat loss to the walls initially increases with the increase in fueling, but subsequently decreases and finally returns to the initial value
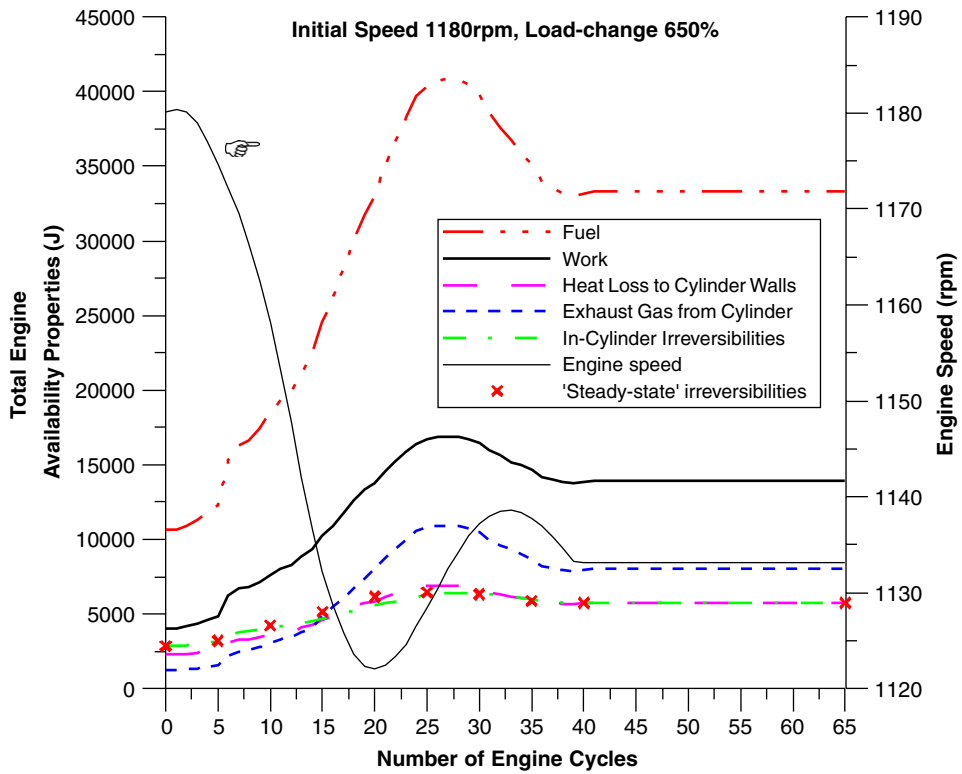
Fig. 2. Response of total availability properties from all six cylinders of the engine to an increase in load.
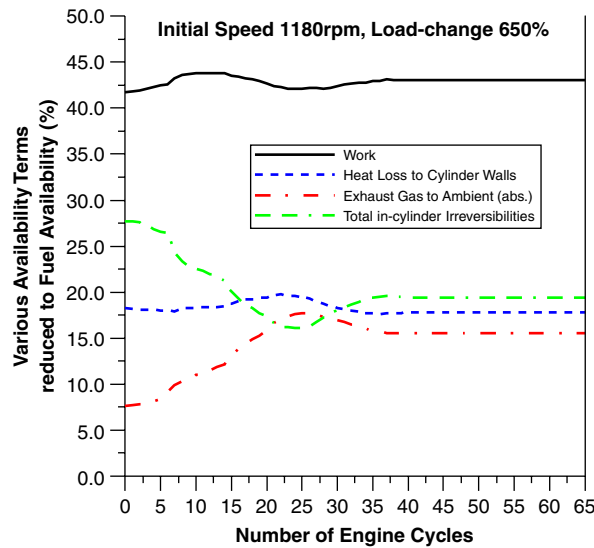

Fig. 3. Response of reduced in-cylinder availability properties to an increase in load.

of almost 18% of the fuel availability, owing to the greater increases of the other terms. The response of the heat loss term shows a hysterysis compared to the work one, although it should be noted that the maximum change in the reduced values is in the order of 2 percentage points, or approximately 10%, compared to the peak value observed at cycle 23. The absolute value of the reduced term of exhaust gases leaving the cylinder

(corresponding mass flow rate $\dot{m}_{2j}$ and flow availability b_{2j} in Eq. (4)), on the other hand, increases steadily with the increase in fueling as the transient event develops. The reduced in-cylinder irreversibilities decrease due to the fact that combustion irreversibilities fall with increasing load. Greater loads result in less degradation of fuel chemical availability when transferred to the (hotter) exhaust gases.

Although the primary application of the present engine is a marine one, it was decided to investigate the effect of various engine-load parameters in order to draw some interesting conclusions that may be projected to other engine applications. In the following diagrams, the effect of five interesting (dynamic, thermodynamic and design) parameters on the engine's first- and second-law transient response is investigated. These are: the type of loading connected to the engine, the turbocharger mass moment of inertia, the cylinder wall temperature, the aftercooler effectiveness and the exhaust manifold volume. For all cases analyzed below, unless otherwise stated, the following assumptions are valid:

(1) The initial load is 10% of the engine's full load at the initial speed of 1180 rpm.
(2) A 650% load change is applied in 1.3 s (real load application time) corresponding roughly to a 10–75% load change.
(3) The loading type is quadratic (hydraulic brake, $s = 2$ in Eq. (12)) corresponding to the propeller law, typical for marine applications with fixed pitch propeller.
(4) The temperature of the cylinder walls ranges from 400 K (at the initial operating point of 10% load) to 500 K (100% loading) in the vicinity of 1180 rpm engine speed, according to the current fueling conditions. This temperature is assumed to remain steady during each cycle, differentiating from cycle to cycle.

In all the following diagrams we will show, as regards first-law properties, the response of engine speed, fuel pump rack position and a third property (such as turbocharger speed or engine load) depending on the examined parameter. As regards second-law properties, the in-cylinder irreversibilities reduced to the fuel availability plus another interesting second-law property, which will depend each time on the examined engine parameter, will be depicted in the same multiple diagram for comparative purposes.

Fig. 4 presents the effect of the type of loading connected to the engine. Here, apart from the nominal case of quadratic loading, the rigid loading ($s = 0$ in Eq. (12)), corresponding to the loading experienced by a car at upward hill climbing and the linear loading ($s = 1$), corresponding to electrical generator set are also examined. The reduced term of the exhaust gas to ambient was chosen as the interesting second-law property along with the reduced in-cylinder irreversibilities. The lower the exponent "s" in Eq. (12), that means a more rigid connected loading, the greater the engine (maximum and final) speed droop (difference between initial and final engine speed), which in turn leads to greater fuel pump rack positions and consequently to an increase in the injected fuel quantity, thus decreasing the in-cylinder irreversibilities reduced to the fuel availability. Consequently, the reduced exhaust gas to ambient availability term, although significantly exploited through the turbocharging system, is greater, increasing the possible work recovery from the exhaust gas, i.e., by means of a bottoming cycle. Since the engine in hand possesses a large moment of inertia and the applied load change of 650% is definitely within the engine's "capability", the differences observed between the three examined resistance types are not great as regards all the depicted properties.

Similar results would be observed if studying the effect of the magnitude of applied load, i.e., a greater applied load resembles a more rigid connected loading.

Fig. 5 investigates the effect of the turbocharger mass moment of inertia on the response of the engine. Two cases are examined apart from the nominal one. In the first case, the T/C inertia is one fifth of the nominal inertia, as it would be the case for vehicular applications, and in the second one its value is 10 times the nominal one that is rather typical for electrical generation applications. The turbocharger speed was chosen here as the third interesting first-law property. The greater the turbocharger mass moment of inertia, the slower the response of the turbocharger, as it is clearly depicted in the turbocharger speed sub-diagram leading to greater values of fuel pump rack and consequently fueling. On the other hand, the lower the turbocharger mass moment of inertia the lower the speed droop due to faster and more abrupt movement of the fuel pump rack, leading to greater in-cylinder irreversibilities and thus lower exhaust gas availability from the cylinder (reduced to the injected fuel chemical availability). However, this occurs, at least for the particular engine, at the expense of a pulsating engine response (with decreasing magnitude) that is, in general, unacceptable.
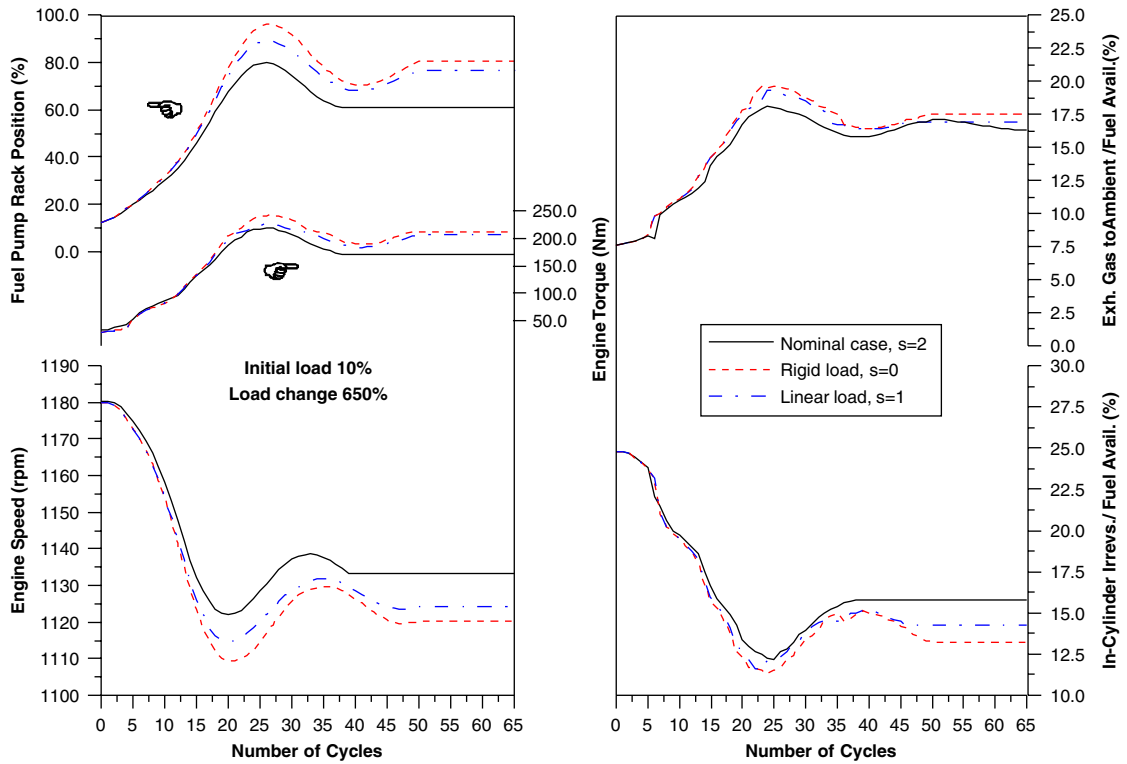
Fig. 4. Comparative first- and second-law properties response, after a ramp increase in load, for various connected load types.
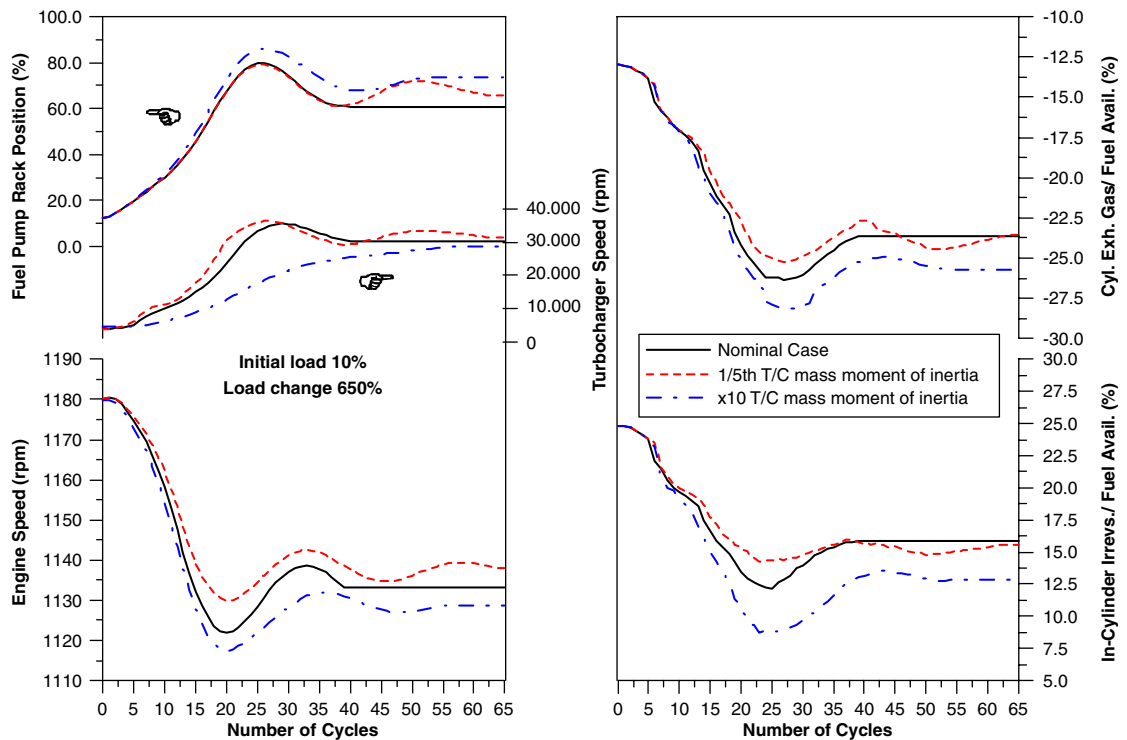

Fig. 5. Comparative first- and second-law properties response, after a ramp increase in load, for various turbocharger mass moments of inertia.
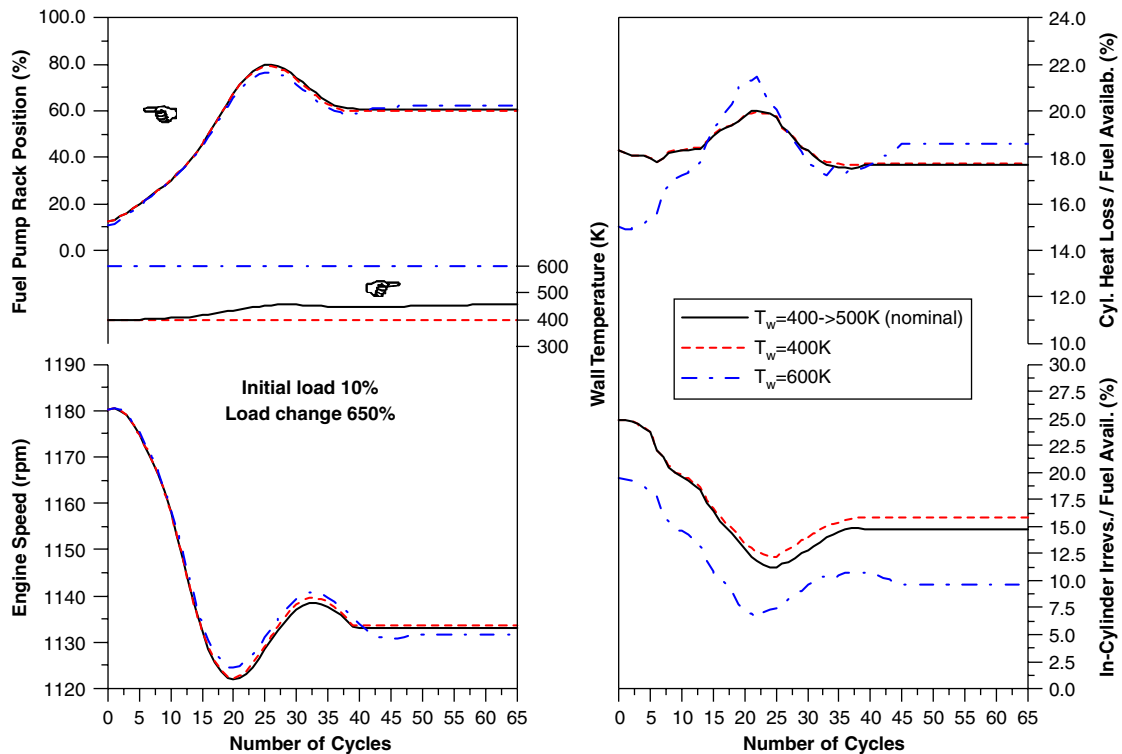
Fig. 6. Comparative first- and second-law properties response, after a ramp increase in load, for various cylinder wall temperature profiles.

Fig. 6 focuses on the effect of the cylinder wall temperature on the response of the engine. The reduced heat loss to the cylinder walls availability was chosen here as the interesting second-law property for depiction, along with the reduced in-cylinder irreversibilities. In the first case, the cylinder wall temperature is 400 K remaining steady throughout the transient event. In the second case (nominal), the wall temperature is assumed to vary from 400 to 500 K according to the engine (steady-state) fueling. Lastly, in the third case, the cylinder wall is assumed to remain steady at 600 K, which resembles the "adiabatic" or low heat rejection engine operation. An increasing wall temperature leads to greater gas temperatures inside the cylinder, which in turn lower the in-cylinder irreversibilities reduced to the fuel availability (cf. Fig. 4), while the availability of the heat loss to the cylinder walls increases both in absolute terms (in Joules) and reduced to the injected fuel availability. Notice that for the "adiabatic" wall case the reduced in-cylinder irreversibilities drop up to 7.5% (at cycle 22) compared to the 12% for the nominal case, denoting how favorable, according to the second-law perspective, this configuration is. Heat losses to the cylinder walls increase accordingly as a result of the reduced combustion irreversibilities, thus highlighting a possible source for work recovery. On the other hand, the cylinder wall temperature effect on the engine speed and the other first-law properties response is minimal. Consequently, there is a (theoretical) significant potential for work recovery during this transient operation, which the first-law analysis cannot reveal.

Fig. 7 investigates the effect of the aftercooler effectiveness on the engine first- and second-law response. Double and half values for the aftercooler effectiveness were chosen here, for the sake of this study. The engine recovery (speed and fuel pump rack position) remains almost unaffected by the magnitude of the aftercooler effectiveness (and thus inlet manifold temperature), a fact, however, not applicable to the second-law properties. Increasing aftercooler effectiveness decreases the charge air temperature, leading to increased reduced in-cylinder irreversibilities due to greater degradation of the fuel availability to "cooler" exhaust gases. Consequently, it is an unfavorable design choice as regards second-law perspective. A difference in the order of 15% is observed at cycle 25 compared to the nominal case.
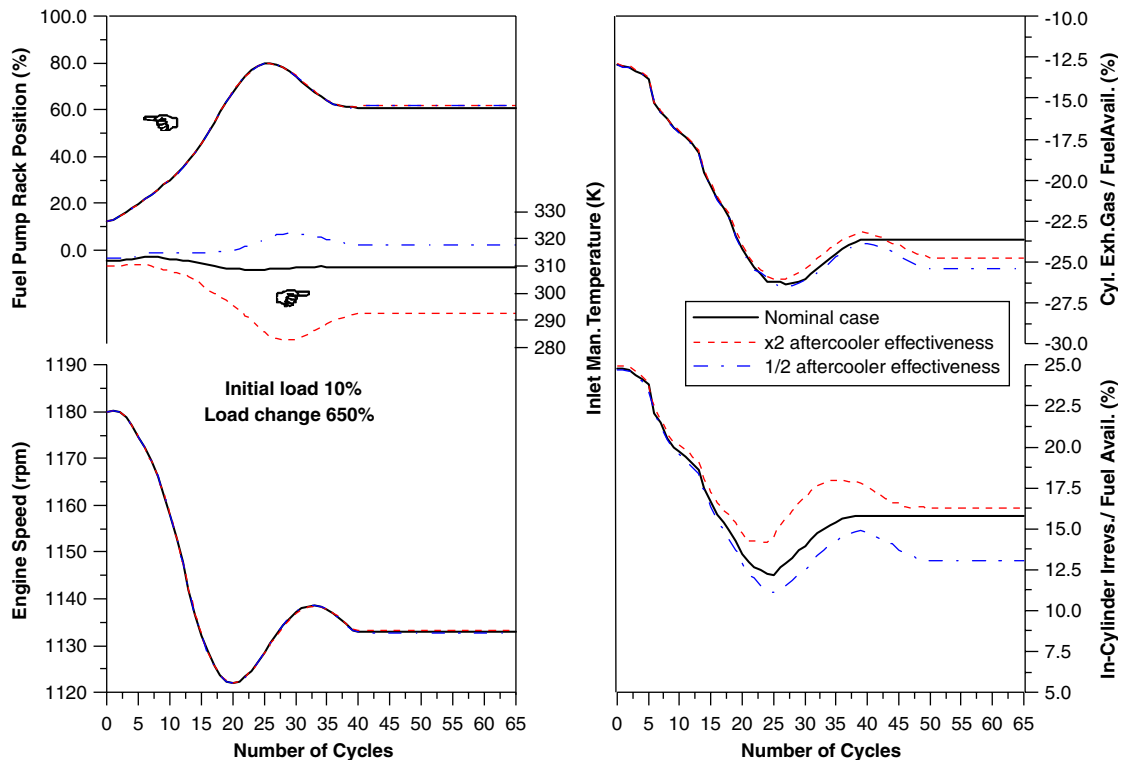
Fig. 7. Comparative first- and second-law properties response, after a ramp increase in load, for various aftercooler effectiveness values.
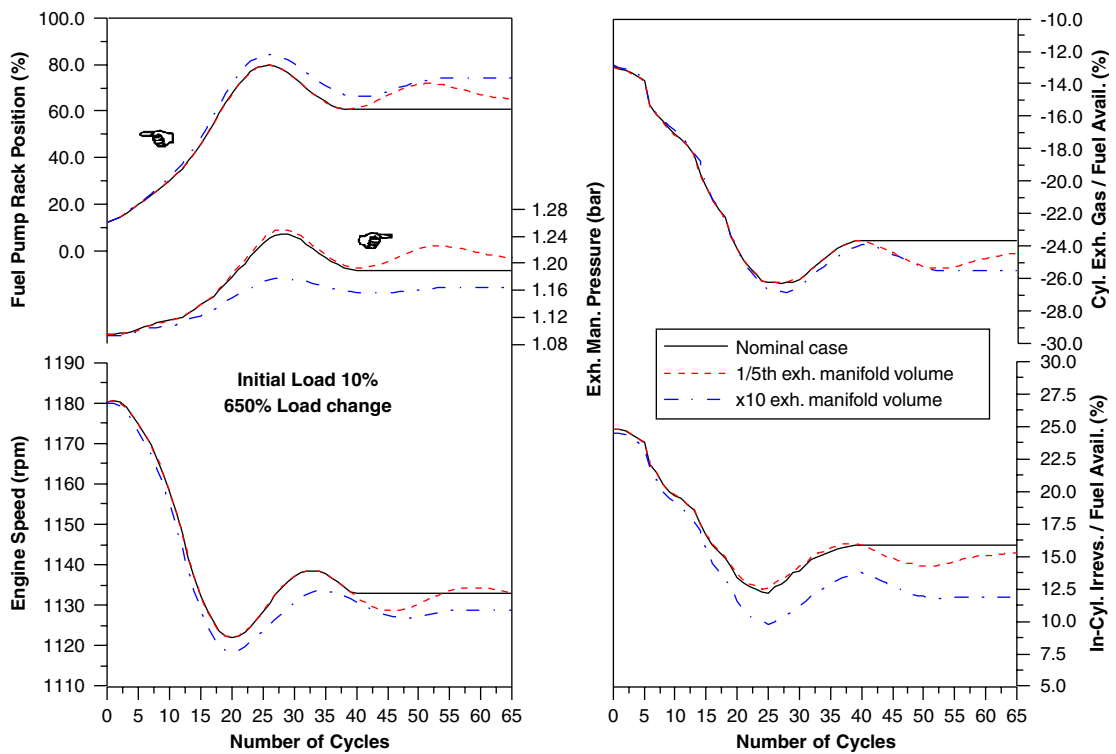

Fig. 8. Comparative first- and second-law properties response, after a ramp increase in load, for various exhaust-manifold volumes.

Finally, Fig. 8 focuses on the effect of the exhaust manifold volume on the engine response. The interesting second-law property is here again the reduced availability of the exhaust gas from the cylinder. As expected, a large exhaust manifold volume (which resembles a constant pressure turbocharging system, typical for large marine diesel engines) leads to slow response of the turbocharger and thus a retarded engine (speed) response as regards both speed droop and recovery period. Moreover, it increases the injected fuel quantity and so decreases the relative importance of the in-cylinder irreversibilities. A much smaller exhaust manifold volume, on the other hand, as it would be the case for vehicle applications, can lead to unsteady and pulsating operation of the particular engine and is thus hardly acceptable. Consequently, a compromise design has to be met for optimum response.

8. Conclusions

A detailed first- and second-law analysis has been carried out on a six-cylinder, turbocharged diesel engine, in order to study the first- and second-law balances of the engine during transient operation, after a load change commencing from a low load. The model's energy results are confirmed with experimental tests. The engine is characterized by a high moment of inertia typical for marine but also stationary (e.g., electrical generation) applications and a narrow speed range that limited the analysis to load changes. Various engine operating parameters effects were studied from both first- and second-law perspectives. The following conclusions were drawn, which are believed to be useful for the study of different engine applications too:

Cylinder irreversibilities account for a significant percentage of the injected fuel availability during a transient event, after a ramp increase in load, though with decreasing importance with increasing load.
Other second-law terms, such as exhaust gas from cylinder or to ambient (although already exploited through the turbocharging system) as well as heat loss to the cylinder walls are of important magnitude, the recovery of which can notably improve engine performance.
All the parameters that lead to slow engine speed recovery (such as large exhaust manifold volume or high T/C mass moment of inertia or high engine mass moment of inertia, which was not studied in this paper) result in similarly slow turbocharger recovery, increased fuel injected quantities and thus decreased in-cylinder irreversibilities and increased exhaust gas from cylinder or to ambient availability (reduced to the fuel availability). They are, therefore, favorable from the second-law perspective since they increase the potential for work recovery using a bottoming cycle.
The recovery period and the general profile of the second-law properties response depend on the respective first-law ones, since the second-law properties are evaluated using first-law data. For the particular engine configuration, which is characterized by a high-mass moment of inertia, all the second-law terms are delayed compared to the engine speed response due to the slow movement of the governor.
The more rigid the connection to the engine-load type is, the greater the in-cylinder irreversibilities (in Joules) though with decreasing reduced value.
A small turbocharger mass moment of inertia causes faster response, but it can lead to pulsating (first- and second-law) recovery which is, in general, not favorable.
The effect of the cylinder wall temperature (profile) is minimal as regards engine first-law equilibrium profile and final conditions, but with significant effect on the reduced in-cylinder irreversibilities.
The effect of the aftercooler effectiveness in the engine first-law transient response is similarly minimal, whereas the second-law terms are significantly affected.
The exhaust manifold volume can markedly affect the engine and turbocharger response after a ramp increase in load, leading even to unsteady and pulsating operation if a very small manifold volume, e.g., as in vehicle applications, is chosen.

It can safely be stated that second-law analysis results do not always go along with the first-law ones, strengthening the belief that a joint first- and second-law optimization may be a very good choice for establishing best engine performance, taking into account the recovery of the wasted heat or exhaust gases through the minimization of the in-cylinder irreversibilities.

References

[1] Horlock JH, Winterbone DE. The thermodynamics and gas dynamics of internal combustion engines, vol. II. Oxford: Clarendon Press; 1986.

[2] Watson N, Marzouk M. A non-linear digital simulation of turbocharged diesel engines under transient conditions. SAE paper no. 770123. Warrendale, PA: Society of Automotive Engineers Inc.; 1977.

[3] Winterbone DE, Benson RS, Mortimer AG, Kenyon P, Stotter A. Transient response of turbocharged diesel engines. SAE paper no. 770122. Warrendale, PA: Society of Automotive Engineers Inc; 1977.

[4] Watson N. Transient performance simulation and analysis of turbocharged diesel engines. SAE paper no. 810338. Warrendale, PA: Society of Automotive Engineers Inc; 1981.

[5] Qiao J, Dent JC, Garner CP. Diesel engine modeling under steady and transient conditions using a transputer based concurrent computer. Trans SAE J Engines 1992;101:1909–30.

[6] Rakopoulos CD, Giakoumis EG, Hountalas DT. A simulation analysis of the effect of governor technical characteristics and type on the transient performance of a naturally aspirated IDI diesel engine. Trans SAE J Engines 1997;106:905–22.

[7] Rakopoulos CD, Giakoumis EG, Hountalas DT. Experimental and simulation analysis of the transient operation of a turbocharged multi-cylinder IDI diesel engine. Energy Res 1998;22:317–31.

[8] Serrano JR, Reyes E, Payri F. A model for load transients of turbocharged diesel engines. SAE paper no. 1999-01-0225. Warrendale, PA: Society of Automotive Engineers Inc; 1999.

[9] Rakopoulos CD, Giakoumis EG, Hountalas DT, Rakopoulos DC. The effect of various dynamic, thermodynamic and design parameters on the performance of a turbocharged diesel engine operating under transient load conditions. SAE paper no. 2004-01-0926. Warrendale, PA: Society of Automotive Engineers Inc; 2004.

[10] Galindo J, Lujan JM, Serrano JR, Dolz V, Guilain S. Design of an exhaust manifold to improve transient performance of a high-speed turbocharged diesel engine. Exp Therm Fluid Sc 2004;28:863–75.

[11] Moran MJ. Availability analysis: a guide to efficient energy use. Englewood Cliffs, NJ: Prentice-Hall; 1982.

[12] Alkidas AC. The use of availability and energy balances in diesel engines. SAE paper no. 890822. Warrendale, PA: Society of Automotive Engineers Inc; 1989.

[13] Bejan A, Tsatsaronis G, Moran M. Thermal design and optimization. New York: Wiley; 1996.

[14] Bozza F, Nocera R, Senatore A, Tuccilo R. Second law analysis of turbocharged engine operation. Trans SAE J Engines 1991;100:547–60.

[15] Dunbar WR, Lior N. Sources of combustion irreversibility. Combustion Sci Technol 1994;103:41–61.

[16] Dunbar WR, Lior N, Gaggioli RA. The component equations of energy and exergy. Trans ASME J Energy Res Technol 1992;114:75–83.

[17] Flynn PF, Hoag KL, Kamel MM, Primus RJ. A new perspective on diesel engine evaluation based on second law analysis. SAE paper no. 840032. Warrendale, PA: Society of Automotive Engineers Inc; 1984.

[18] Van Gerpen JH, Shapiro HN. Second-law analysis of diesel engine combustion. Trans ASME J Eng Gas Turbines Power 1990;112:129–37.

[19] Rakopoulos CD, Giakoumis EG. Development of cumulative and availability rate balances in a multi-cylinder turbocharged IDI diesel engine. Energy Convers Manage 1997;38:347–69.

[20] Gallo WLR, Milanez LF. Exergetic analysis of ethanol and gasoline fueled engines. SAE paper no. 920809. Warrendale, PA: Society of Automotive Engineers Inc; 1992.

[21] Primus RJ, Hoag KL, Flynn PF, Brands MC. An appraisal of advanced engine concepts using second law analysis techniques. SAE paper no. 841287. Warrendale, PA: Society of Automotive Engineers Inc; 1984.

[22] Alkidas AC. Performance and emissions achievements with an uncooled, heavy-duty single-cylinder diesel engine. SAE paper no. 890144. Warrendale, PA: Society of Automotive Engineers Inc; 1989.

[23] Caton JA. On the destruction of availability (exergy) due to combustion processes with specific application to internal combustion engines. Energy 2000;25:1097–117.

[24] Kyritsis DC, Rakopoulos CD. Parametric study of the availability balance in an internal combustion engine cylinder. SAE paper no. 2001-01-1263. Warrendale, PA: Society of Automotive Engineers Inc; 2001.

[25] Nakonieczny K. Entropy generation in a diesel engine turbocharging system. Energy 2002;27:1027–56.

[26] Rakopoulos CD, Giakoumis EG. Simulation and exergy analysis of transient diesel-engine operation. Energy 1997;22:875–85.

[27] Rakopoulos CD, Giakoumis EG. Availability analysis of a turbocharged diesel engine operating under transient load conditions. Energy 2004;29:1085–104.

[28] Rakopoulos CD, Giakoumis EG. Parametric study of transient turbocharged diesel engine operation from the second-law perspective. SAE paper no. 2004-01-1679. Warrendale, PA: Society of Automotive Engineers Inc; 2004.

[29] Heywood JB. Internal combustion engine fundamentals. New York: McGraw-Hill; 1988.

[30] Benson RS, Whitehouse ND. Internal combustion engines. Oxford: Pergamon Press; 1979.

[31] Rakopoulos CD, Hountalas DT. Development and validation of a 3-D multi-zone combustion model for the prediction of DI diesel engines performance and pollutants emissions. Trans SAE J Engines 1998;107:1413–29.

[32] Rakopoulos CD, Hountalas DT. Development of new 3-D multi-zone combustion model for indirect injection diesel engines with a swirl type prechamber. Trans SAE J Engines 2000;109:718–33.

[33] Hiroyasu H, Kadota T, Arai M. Development and use of a spray combustion modeling to predict diesel engine efficiency and pollutant emissions. Bull JSME 1983;26:569–76.

[34] Annand WJD. Heat transfer in the cylinders of reciprocating internal combustion engines. Proc Inst Mech Eng 1963;177: 983–90.

[35] Rezeka SF, Henein NA. A new approach to evaluate instantaneous friction and its components in internal combustion engines. SAE paper no. 840179. Warrendale, PA: Society of Automotive Engineers Inc; 1984.

[36] Kouremenos DA, Rakopoulos CD, Hountalas DT, Kotsiopoulos PN. A simulation technique for the fuel injection system of diesel engines. Proceedings of the ASME-WAM, AES, Atlanta, GA, vol. 24, 1991. p. 91–102.